Self-consistent generalized Langevin equation theory of the dynamics of multicomponent atomic liquids

Edilio Lázaro-Lázaro, Patricia Mendoza-Méndez, Luis Fernando Elizondo-Aguilera, Jorge Adrián Perera-Burgos, Pedro Ezequiel Ramírez-González, Gabriel Pérez-Ángel, Ramón Castañeda-Priego, and Magdaleno Medina-Noyola

Citation: The Journal of Chemical Physics **146**, 184506 (2017); doi: 10.1063/1.4983217
View online: http://dx.doi.org/10.1063/1.4983217
View Table of Contents: http://aip.scitation.org/toc/jcp/146/18
Published by the American Institute of Physics

Self-consistent generalized Langevin equation theory of the dynamics of multicomponent atomic liquids

Edilio Lázaro-Lázaro,[1] Patricia Mendoza-Méndez,[1] Luis Fernando Elizondo-Aguilera,[2,3] Jorge Adrián Perera-Burgos,[4] Pedro Ezequiel Ramírez-González,[5] Gabriel Pérez-Ángel,[6] Ramón Castañeda-Priego,[2] and Magdaleno Medina-Noyola[1,2]

[1]*Instituto de Física "Manuel Sandoval Vallarta," Universidad Autónoma de San Luis Potosí, Álvaro Obregón 64, 78000 San Luis Potosí, SLP, Mexico*
[2]*Departamento de Ingeniería Física, División de Ciencias e Ingenierías, Universidad de Guanajuato, Loma del Bosque 103, 37150 León, Mexico*
[3]*Institut für Materialphysik im Weltraum, Deutsches Zentrum für Luft-und Raumfahrt (DLR), 51170 Köln, Germany*
[4]*Facultad de Química, Universidad Autónoma del Carmen, C. 56 No. 4 Esq. Avenida Concordia, Col. Benito Juárez, C.P., 24180 Cd. del Carmen, Campeche, Mexico*
[5]*CONACYT- Instituto de Física "Manuel Sandoval Vallarta," Universidad Autónoma de San Luis Potosí, Álvaro Obregón 64, 78000 San Luis Potosí, SLP, México*
[6]*Departamento de Física Aplicada, Cinvestav, Unidad Mérida, Apartado Postal 73 Cordemex, 97310 Mérida, Yucatán, Mexico*

(Received 10 January 2017; accepted 27 April 2017; published online 12 May 2017)

A fundamental challenge of the theory of liquids is to understand the similarities and differences in the macroscopic dynamics of both colloidal and atomic liquids, which originate in the (Newtonian or Brownian) nature of the microscopic motion of their constituents. Starting from the recently discovered long-time dynamic equivalence between a colloidal and an atomic liquid that share the same interparticle pair potential, in this work we develop a self-consistent generalized Langevin equation theory for the dynamics of equilibrium multicomponent atomic liquids, applicable as an approximate but quantitative theory describing the long-time diffusive dynamical properties of simple equilibrium atomic liquids. When complemented with a Gaussian-like approximation, this theory is also able to provide a reasonable representation of the passage from a ballistic to diffusive behavior. We illustrate the applicability of the resulting theory with three particular examples, namely, a monodisperse and a polydisperse monocomponent hard-sphere liquid and a highly size-asymmetric binary hard-sphere mixture. To assess the quantitative accuracy of our results, we perform event-driven molecular dynamics simulations, which corroborate the general features of the theoretical predictions. *Published by AIP Publishing.* [http://dx.doi.org/10.1063/1.4983217]

I. INTRODUCTION

It is well known that the structural and dynamical properties of atomic liquids[1–4] and colloidal fluids[5–7] exhibit an almost perfect correspondence.[8,9] It is not difficult to understand[10–12] why the equilibrium thermodynamic and structural properties of a specific model system (say a Lennard-Jones liquid) will be independent of the microscopic (either molecular or Brownian) dynamics that govern the motion of the N interacting particles that constitute the system. In contrast, the dynamic properties of the same systems are expected in general to depend on the specific microscopic dynamics.[13–15] From the theoretical side, one would like to understand the microscopic origin of the similarities and differences in the macroscopic dynamics of colloidal and atomic liquids within a common unifying theoretical framework. In fact, this problem has been addressed theoretically and with simulations in the context of the long-time dynamics of Newtonian and Brownian systems near the glass transition.[16–20] A number of issues, however, still remain open.

In a recent contribution,[21] the generalized Langevin equation (GLE) formalism[22] was employed to derive the exact equation of motion of individual tracer particles,[23] as well as the exact time-evolution equations for both collective and self-intermediate scattering functions, $F(k, t)$ and $F_S(k, t)$, respectively, of an atomic liquid,[24] with k being the magnitude of the wavevector. A remarkable fundamental consequence of these theoretical results is the general prediction that, properly scaled, the strictly *long-time* dynamics of an atomic liquid should be indistinguishable from the dynamics of the Brownian liquid with the same interparticle interactions. This prediction has been successfully tested by computer simulations.[23–25]

The first main purpose of the present work is to adapt now the arguments and approximations previously employed in the proposal of the approximate self-consistent generalized Langevin equation (SCGLE) theory of *colloid* dynamics and dynamical arrest,[26] to convert the exact results for tracer diffusion in Ref. 23 and for $F(k, t)$ and $F_S(k, t)$ in Ref. 24, into an approximate theory for the *long-time* dynamic properties of a monocomponent atomic liquid. The expectation is that the resulting atomic extension of the SCGLE theory will provide a unifying theoretical framework to describe in more detail the most relevant similarities and differences

between the macroscopic dynamics of atomic and colloidal liquids (in the absence of hydrodynamic interactions). This implies that in general, if the dynamical properties of a Brownian fluid whose molecules interact with a given interaction potential have been explicitly determined, then one has automatically determined the long-time dynamics of its equivalent atomic system. This, however, involves the proper determination[21] of the "short-time" self-diffusion coefficient D^0 of the atomic liquid by simple random-flight and kinetic-theoretical arguments.[10]

Although irrelevant for the study of phenomenology such as the slow dynamics of glass-forming liquids, a conceptually important issue is the difference in the short-time dynamics of colloidal and atomic liquids: the dynamics of the former is diffusive at all relevant time scales, whereas the dynamics of the latter crosses over from ballistic to diffusive after a few particle collisions. Thus, a secondary aim of this paper is to show how this SCGLE theory for the long-time dynamics of atomic liquids may be complemented with a short-time Gaussian approximation in order to provide a reasonable and simple representation of the passage from a ballistic to diffusive behavior of the mean-square displacement and the intermediate scattering functions of the atomic liquid. With the aim of testing the main features and the quantitative accuracy of the resulting "first principles" approximate theory of the dynamics of atomic liquids, in this paper we also present the results of a set of event-driven molecular dynamics simulations for the hard-sphere model liquid.

The second main purpose of this paper is to use the multicomponent extension of the SCGLE theory of colloid dynamics[27,28] to further extend the SCGLE theory of the dynamics of monoatomic liquids just described, now to *mixtures* of *atomic* liquids. This opens the possibility to model the dynamics of a large class of scientifically and technologically relevant systems and materials, many of which present interesting glass-forming properties. In this regard, let us emphasize that the present multicomponent SCGLE theory shares these aims with the well-known mode coupling theory (MCT) of the ideal glass transition[29,30] and its multi-component extension.[31–33] In fact, many of the predictions of MCT have been checked in experiments as well as computer simulations and it was found that MCT is indeed able to give a correct description of the initial slowdown of real and simulated supercooled liquids.[34–36]

Unfortunately, MCT and SCGLE theory are strictly theories of the dynamic properties of liquids in thermodynamic equilibrium. Thus, they are unable to predict the most interesting and essential non-equilibrium features of glassy states, such as aging, and the dependence of the properties of glassy materials on their preparation protocol.[37] The SCGLE theory, however, was recently extended to genuine non-equilibrium conditions,[38] thus contributing to demolish this severe limitation. In its first applications, the resulting *non-equilibrium* self-consistent generalized Langevin equation (NE-SCGLE) theory of irreversible processes in liquids has exhibited a remarkable predictive power, particularly in setting the description of the kinetics of the aging of glasses and gels in the same conceptual framework using simple Lennard-Jones-like benchmark models.[39,40] Applying this new non-equilibrium theory to multicomponent atomic liquids, however, has as a prerequisite the previous development of the equilibrium version of the SCGLE theory, and this provides another fundamental reason for our present study, which will thus be strictly confined to equilibrium conditions.

In order to test the reliability of our proposed SCGLE theory, here we also compare its predictions with the results of our event-driven molecular dynamics simulation involving two illustrative applications: a polydisperse hard sphere (HS) liquid, modeled as a moderately size-asymmetric binary HS mixture, and a genuine, highly size-asymmetric, binary HS mixture. As the corresponding comparisons indicate, the present equilibrium SCGLE theory of the dynamics of multicomponent atomic liquids does provide the correct qualitative features and a very acceptable quantitative description of the dynamics of these systems.

This manuscript is organized as follows. In Section II, the main results of the derivation of three general time-evolution equations are summarized. In the same section, we also introduce those approximations that transform these equations into a fully self-consistent system of equations for the overdamped dynamics of a monocomponent atomic liquid. As mentioned above, such overdamped SCGLEs do not describe properly the ballistic behavior of the atomic liquid. Thus, in Sec. III, a simple approximation to fully account for the ballistic regime is explored within the so-called Gaussian approximation; this approach will allow us to describe the passage time of $F_S(k,t)$ and the mean squared displacement (MSD) from the ballistic to the diffusive time regime. Although the results described in Sections II and III are only applicable to monocomponent atomic liquids, the multicomponent extension of the SCGLE theory for the dynamics of atomic liquids is presented in Section IV. The predictions of the resulting SCGLE theory for both monocomponent and multicomponent atomic liquids are discussed and compared in detail with event-driven computer simulations in Sections III and IV, respectively. The main conclusions of this work are finally summarized in Sec. V.

II. REVIEW OF THE TRACER, COLLECTIVE, AND SELF-DIFFUSION IN *MONOCOMPONENT* ATOMIC LIQUIDS

In this section, we briefly review the main concepts and results of Refs. 23 and 24, upon which we build the approximate SCGLE theory of the *long-time* dynamics of *monocomponent* atomic liquids. As we mentioned in the Introduction, in Ref. 23 the generalized Langevin equation formalism[22] was applied to derive the stochastic time-evolution equation for the velocity $\mathbf{v}(t)$ that describes the Brownian motion of individual tracer particles in an atomic liquid. In Ref. 24, general memory-function equations were derived for the intermediate scattering functions (ISFs) $F(k,t)$ and $F_S(k,t)$, which describe the collective and self motion, respectively, of atomic liquids. The overdamped version of these exact equations is formally identical to the corresponding equations of a Brownian liquid. Therefore, in this section, we introduce the same approximations employed before in the construction of the approximate SCGLE theory of Brownian liquids[26] in order to build the

SCGLE theory for the long-time dynamics of monocomponent atomic liquids.

A. Brownian motion of atomic tracers

Let us consider a simple atomic fluid formed by N identical spherical particles in a volume V at a temperature T, whose microscopic dynamics is described by Newton's equations,

$$M\frac{d\mathbf{v}_\alpha(t)}{dt} = \sum_{\beta\neq\alpha}\mathbf{F}_{\alpha\beta}(t), \quad (\alpha = 1, 2, \ldots, N), \tag{2.1}$$

where M is the mass and $\mathbf{v}_\alpha(t) = d\mathbf{r}_\alpha(t)/dt$ the velocity of the αth particle at position $\mathbf{r}_\alpha(t)$, and in which the interactions between the particles are represented by the sum of the pairwise forces, with $\mathbf{F}_{\alpha\beta} = -\nabla_\alpha u(|\mathbf{r}_\alpha - \mathbf{r}_\beta|)$ being the force exerted on particle α by particle β and $u(|\mathbf{r}_\alpha - \mathbf{r}_\beta|)$ the pair potential among particles. In Ref. 23, the general aim was to establish a connection between the microscopic dynamics described by these (Newton's) equations and the macroscopic dynamical properties of the atomic fluid.

The main result of Ref. 23 is the derivation of the generalized Langevin equation that describes the ballistic-to-diffusive crossover of a tagged particle in the atomic liquid. Such stochastic equation reads as

$$M\frac{d\mathbf{v}(t)}{dt} = -\zeta^0\mathbf{v}(t) + \mathbf{f}^0(t) - \int_0^t dt'\Delta\zeta(t-t')\mathbf{v}(t') + \mathbf{F}(t). \tag{2.2}$$

In this equation, the random force $\mathbf{f}^0(t)$ is a "white" noise, i.e., a delta-correlated, stationary, and Gaussian stochastic process with zero mean and time-dependent correlation function given by $\overline{\mathbf{f}^0(t)\mathbf{f}^0(t')} = \overleftrightarrow{\mathbf{I}}\ k_BT\zeta^0 2\delta(t-t')$, with $\overleftrightarrow{\mathbf{I}}$ being the 3×3 Cartesian unit tensor and k_BT the thermal energy. The term involving the time-dependent friction function $\Delta\zeta(t)$ describes the average dissipative friction effects due to the conservative (or "direct") forces on the tracer particle, whose random component is the stationary stochastic force $\mathbf{F}(t)$ that obeys the fluctuation-dissipation relationship $\overline{\mathbf{F}(t)\mathbf{F}(t')} = \overleftrightarrow{\mathbf{I}}\ k_BT\Delta\zeta(t-t')$. Thus, the configurational effects of the interparticle interactions are embodied in the time-dependent friction function $\Delta\zeta(t)$, for which the following approximate expression was also derived in Ref. 23:

$$\Delta\zeta(t) = \frac{k_BT}{3(2\pi)^3 n}\int d\mathbf{k}\left[\frac{k[S(k)-1]}{S(k)}\right]^2 F(k,t)F_S(k,t), \tag{2.3}$$

where $n \equiv N/V$ is the number density and $S(k)$ is the static structure factor.

Eqs. (2.2) and (2.3), valid for an atomic liquid, turn out to be formally identical to the corresponding results derived in Ref. 22 for a Brownian liquid in the absence of hydrodynamic interactions, see, e.g., Eqs. (4.9) and (4.10) of Ref. 22. The most remarkable conclusion of Ref. 23 is that the Brownian motion of any labeled particle in an atomic liquid is formally described by the same equation that describes the Brownian motion of a labeled particle in a liquid of interacting colloidal particles, provided both liquids share the same thermodynamic conditions and their molecular constituents interact with the same pair potential. The fundamental difference between these two dynamically distinct systems lies in the physical origin of the friction force $-\zeta^0\mathbf{v}(t)$ and in the determination of the friction coefficient ζ^0: in a colloidal liquid the friction force $-\zeta^0\mathbf{v}(t)$ is caused by the supporting solvent, and hence, ζ^0 assumes its Stokes value.[10] In contrast, the friction force $-\zeta^0\mathbf{v}(t)$ in an atomic liquid is not caused by any external material agent, instead, its origin is a more subtle kinetic mechanism,[21] which originates in the spontaneous tendency to maintain the equipartition of kinetic energy through molecular collisions. Uhlenbeck and Ornstein refer to this effect as "*Doppler*" friction, caused by the fact that when any tracer particle of the fluid "*is moving, say to the right, it will be hit by more molecules from the right than from the left.*"[41] These collisional effects are described by the kinetic friction coefficient ζ^0 which, according to Refs. 21 and 23, is defined through Einstein's relation,

$$\zeta^0 \equiv k_BT/D^0, \tag{2.4}$$

with the short-time self-diffusion coefficient D^0 determined by the same arguments employed in the elementary kinetic theory of gases.[10] According to such arguments, the mean free path l_0 can be approximated as $l_0 \approx 1/n\sigma_{col}^2$, with σ_{col} being the collision diameter of the atoms. The diffusion coefficient that results from a large number of successive collisions is thus given by $D^0 = l_0^2/\tau_0$, where τ_0 is the mean free time, related to l_0 by $l_0/\tau_0 = v_0 \equiv \sqrt{k_BT/M}$. The resulting value of D^0 is given by[10]

$$D^0 \equiv \frac{3}{8}\left(\frac{k_BT}{\pi M}\right)^{1/2}\frac{1}{n\sigma_{col}^2}. \tag{2.5}$$

B. Collective and self-diffusion in atomic liquids

In Ref. 24, the GLE formalism[22] was also employed to derive the exact time-evolution equations for the collective and self intermediate scattering functions, $F(k,t)$ and $F_S(k,t)$, of an atomic liquid in terms of the corresponding memory functions, see, e.g., Eqs. (32) and (33) of Ref. 24. For times t sufficiently long compared with τ_0, i.e., the so-called "overdamped" limit, and in terms of the corresponding Laplace transforms $F(k,z)$ and $F_S(k,z)$, these equations read as (see, e.g., Eqs. (37) and (38) of Ref. 24)

$$F(k,z) = \frac{S(k)}{z + \frac{k^2S^{-1}(k)D^0}{1+C(k,z)}} \tag{2.6}$$

and

$$F_S(k,z) = \frac{1}{z + \frac{k^2D^0}{1+C_S(k,z)}}, \tag{2.7}$$

where $C(k,z)$ and $C_S(k,z)$ are the corresponding collective and self memory functions, respectively.[24]

As in the description for colloidal liquids,[42] $C(k,z)$ and $C_S(k,z)$ can be written in terms of the higher-order memory functions $L_{UU}(k,z)$ and $L_{UU}^{(S)}(k,z)$, which are the time-dependent correlation function of the configurational component of the stress tensor.[24] The inclusion of such higher-order memory functions is only necessary if an accurate description of the short-time dynamics becomes a priority. Our present interest, however, refers primarily to the opposite time regime, i.e., the long-time dynamics, which becomes relevant,

for example, for the phenomenology of the glass transition, in which case we may refer only to the primary memory functions $C(k, t)$ and $C_S(k, t)$.

The explicit comparison of the resulting equations for $F(k, z)$ and $F_S(k, z)$ for atomic liquids with those of a colloidal liquid (Eqs. (4.24) and (4.33) of Ref. 42) reveals the remarkable formal identity between the long-time expressions for $F(k, t)$ and $F_S(k, t)$ of an atomic liquid and the corresponding results for the equivalent colloidal system. Analogously, to accurately describe the transition from the ballistic regime to the diffusive behavior, the fundamental difference between both types of liquids turns out to be found in the definition of the diffusion coefficient D^0, given by Eq. (2.5) in the case of atomic liquids.

C. Self-consistent description of the *long-time* dynamics of atomic liquids

The formal identity with the dynamics of Brownian liquids, theoretically predicted in Refs. 23 and 24, immediately suggests that the long-time dynamic properties of an atomic liquid will then coincide with the corresponding properties of a colloidal system with the same $S(k)$, provided that the time is scaled as $D^0 t$ with the respective meaning and definition of D^0. As mentioned before, this expectation has been nicely confirmed by performing both Brownian Dynamics (BD) and Molecular Dynamics (MD) simulations on the same prescribed model system and then comparing the results of both simulations with the appropriate rescaling, see, e.g., Fig. 1 of Ref. 23 and Fig. 2(a) of Ref. 24.

Thus, Eqs. (2.3), (2.6), and (2.7) provide the basis of a theory for the long-time dynamics of atomic liquids. The simplest approximation to close this set of equations is exactly the same as that employed in the SCGLE theory of colloid dynamics.[26] Hence, let us notice that Eq. (2.3) writes $\Delta\zeta^*(t)$ in terms of $F(k, z)$ and $F_S(k, z)$, whereas Eqs. (2.6) and (2.7) describe $F(k, z)$ and $F_S(k, z)$ in terms of the corresponding memory functions $C(k, t)$ and $C_S(k, t)$. Thus, in order to construct a closed system of equations, we now need two independent expressions for $C(k, t)$ and $C_S(k, t)$. The first such major approximation, referred to as the vineyard-like approximation, consists of assuming the simplest connection between $C(k, z)$ and $C_S(k, z)$, namely,[26]

$$C(k, z) \cong C_S(k, z). \tag{2.8}$$

The second major approximation consists of interpolating $C_S(k, z)$ between its two exact limits at small and large wavevectors by means of a completely empirical interpolating function $\lambda(k)$, chosen such that $\lambda(k \to 0) = 1$ and $\lambda(k \to \infty) = 0$. The large wave-vector limit, $C_S(k \to \infty, t)$, is a rapidly decaying function of time, and hence we approximate it by its vanishing long-time value. Thus, one can write $C_S(k, t)$ simply as $C_S(k, t) = \lambda(k) C_S(k = 0, t)$, or as

$$C_S(k, z) = \lambda(k)\Delta\zeta^*(t), \tag{2.9}$$

since one can demonstrate that $C_S(k = 0, t) = \Delta\zeta^*(t)$.

If one now incorporates both vineyard-like and interpolation approximations in Eqs. (2.6) and (2.7), one can then rewrite such equations as

$$F(k, z) = \frac{S(k)}{z + \frac{k^2 D^0 S^{-1}(k)}{1 + \lambda(k)\Delta\zeta^*(t)}} \tag{2.10}$$

and

$$F_S(k, z) = \frac{1}{z + \frac{k^2 D^0}{1 + \lambda(k)\Delta\zeta^*(t)}}, \tag{2.11}$$

with D^0 given by the kinetic value provided in Eq. (2.5). This set of equations together with Eq. (2.3) for $\Delta\zeta^*(t)$ constitutes the closed system of equations that define the self-consistent theory of the long-time dynamics of an atomic liquid. For the interpolating function, the same functional form as in the colloidal case is adopted, namely,

$$\lambda(k) \equiv \frac{1}{1 + \left(\frac{k}{k_c}\right)^2}, \tag{2.12}$$

with k_c being an empirically chosen cutoff wavevector, sometimes related with the position of the maximum k_{max} of $S(k)$ by $k_c = a k_{max}$, with $a > 0$ being the only free parameter, determined by a calibration procedure.[43]

In summary, Eqs. (2.3), (2.5), and (2.10)-(2.12) constitute a self-consistent system of equations for the time-dependent friction function $\Delta\zeta^*(t)$ and the correlation functions $F(k, t)$ and $F_S(k, t)$ of an atomic liquid in the long-time (or overdamped) regime. These equations provide an approximate first-principles prediction of the *diffusive* dynamics of an atomic liquid, i.e., outside the short-time or ballistic regime. They are, however, formally identical to the SCGLE theory of colloid dynamics,[26] and hence, they express the aforementioned dynamical equivalence between atomic and colloidal systems discussed in detail in Refs. 23–25. This predicted long-time dynamical equivalence is best illustrated in terms of the mean squared displacement (MSD), $W(t) \equiv (1/6)\langle(\Delta\mathbf{R}(t))^2\rangle$, which in the case of Brownian liquids is the solution of the following equation:

$$W(t) = D^0 t - \int_0^t \Delta\zeta^*(t - t')W(t)dt' \tag{2.13}$$

and whose long-time limit provides a master curve for both atomic and Brownian liquids, as explicitly illustrated in Section III.

III. CROSSOVER FROM BALLISTIC TO DIFFUSIVE DYNAMICS

The self-consistent set of equations proposed in Sec. II C is sufficient to describe the long-time dynamics of an atomic liquid. Let us now complement this dynamic framework with additional approximations to allow the incorporation of the ballistic short-time behavior. There are, of course, more than one concrete manners to carry out this task, and here, we propose one based on the criterion of analytic and numerical simplicity also on physical self-consistency. Although the ultimate interest in this paper refers to the description of multicomponent atomic liquids, for the sake of the discussion we shall address this issue first in the context of monocomponent systems. The extension to mixtures will be discussed in Sec. III A.

A. *Monocomponent* atomic SCGLE theory

To incorporate the correct short-time limit in the framework of the atomic SCGLE theory, our strategy is to obtain first an accurate description of the crossover from ballistic to diffusive dynamics, well known and typically observed in the MSD, $W(t)$. To this end, let us notice that the exact equation for $W(t)$, which can be directly derived from Eq. (2.2), reads as

$$\tau^0 \frac{dW(t)}{dt} + W(t) = D^0 t - \int_0^t \Delta\zeta^*(t-t')W(t')dt', \tag{3.1}$$

where $\tau^0 \equiv M/\zeta^0 = D^0/v_0^2$. This exact equation can be now closed with the overdamped approximation for the friction function $\Delta\zeta^*(t)$ that results from the solution of Eqs. (2.3), (2.5), and (2.10)-(2.12). Even though this approximation is only valid for $t \gg \tau_0$, at short times, the effects of the interparticle interactions on $W(t)$ (embodied in $\Delta\zeta^*(t)$) are negligible. Nevertheless, the correct short-time ballistic behavior of $W(t)$ is guaranteed by the presence of the first ("inertial") term of Eq. (3.1). Thus, the solution of this equation for $W(t)$ will provide an accurate interpolation between its ballistic (short-time) and long-time (diffusive) regimes, described, respectively, by the following asymptotic limits:

$$W(t) \approx \frac{1}{2} v_0^2 t^2, \text{ for } t \to 0, \tag{3.2}$$

where $v_0^2 \equiv k_B T/M$ and

$$W(t) \approx D_L t, \text{ for } t \to \infty, \tag{3.3}$$

with D_L being the long-time self-diffusion coefficient, determined by the Green-Kubo relation $D_L = \int_0^\infty dt V(t) = V(z=0)$ and by the velocity autocorrelation function $V(t)$, which is obtained from Eq. (2.2) in terms of $\Delta\zeta(t)$, leading to

$$D_L = \frac{D^0}{1+\Delta\zeta^*}, \tag{3.4}$$

with

$$\Delta\zeta^* \equiv \int_0^\infty \left[\frac{\Delta\zeta(t)}{\zeta^0}\right] dt. \tag{3.5}$$

The most natural analogous procedure to incorporate the ballistic regime in the ISFs would be to start with the exact expressions provided in Eqs. (32) and (33) of Ref. 24, in order to introduce general closure relations for the respective memory functions to construct a self-consistent scheme. In fact, we have followed such a kind of procedure and found that the structure of the resulting equations, which naturally should describe the crossover from the ballistic and diffusive limits, sometimes introduced a spurious oscillatory time dependence of the ISFs. This is due to the fact that the analytic structure of such equations is actually not consistent with the Gaussian limit of the ISFs, which is exact at short-times and low particle densities. Although we might attempt to carry out a formal derivation to sort out these difficulties, we have found a simplified alternative which is consistently starting from the overdamped approximations for the ISFs in Eqs. (2.10) and (2.11) to interpolate between the two (short- and long-time) limits of these dynamical properties.

Thus, let us recall now that the well-known Gaussian approximation for $F_S(k,t)$ and $F(k,t)$ defined as[1]

$$F_S(k,t) = e^{-k^2 W(t)} \tag{3.6}$$

and

$$F(k,t) = S(k) e^{-k^2 W(t)/S(k)}. \tag{3.7}$$

As was illustrated in Fig. 2 of Ref. 24, the validity of these approximations is restricted to the short-time regime, $t \lesssim \tau_0$, whereas the solution for Eqs. (2.10) and (2.11) (which from now on will be labeled with a superscript D, i.e., $F^D(k,t)$ and $F_S^D(k,t)$, to denote the solution at long times) correctly describes the value of the ISFs in the complementary time domain, $t \gtrsim \tau_0$. Hence, as a simple description of the ballistic-to-diffusive crossover of the ISFs, we may propose to approximate $F(k,t)$ and $F_S(k,t)$ of an atomic liquid as the following simple exponential interpolation between the two aforementioned limits, namely,

$$F(k,t) = F^D(k,t) + \{S(k)\exp[-k^2 W(t)/S(k)] - F^D(k,t)\}\exp[-t/\tau^0] \tag{3.8}$$

and

$$F_S(k,t) = F_S^D(k,t) + \{\exp[-k^2 W(t)] - F_S^D(k,t)\}\exp[-t/\tau^0]. \tag{3.9}$$

In summary, we have proposed an approximate, but general, first-principles SCGLE theory for the dynamical properties of a simple monocomponent atomic liquid. This theory is finally outlined by Eqs. (2.3), (2.10)-(2.12), (3.1), (3.8), and (3.9), which provide a protocol to determine the dynamical features of an atomic liquid starting from the intermolecular forces, represented by the pair interaction potential $u(r)$. This protocol is now spelled out and illustrated with a specific application.

B. Atomic hard sphere liquid

Once the pair potential $u(r)$ is specified, the first step is to determine the static structure factor $S(k)$ according to any equilibrium (exact or approximate) method. For example, for the atomic version of a liquid of hard spheres (HSs) of diameter σ and number density n, one can approximate $S(k)$ by its analytic Percus-Yevick-Verlet-Weis (PYVW) expression,[44,45] which is highly accurate throughout the stable liquid regime. Using this $S(k)$ as an input, Eqs. (2.3) and (2.10)-(2.12), with $k_c = 8.2$, are solved to determine $\Delta\zeta^*(t)$ and the overdamped ISFs $F^D(k,t)$ and $F_S^D(k,t)$. The resulting $\Delta\zeta^*(t)$ is then employed in Eq. (3.1), whose solution for $W(t)$ provides the input of the expressions in Eqs. (3.8) and (3.9) for $F(k,t)$ and $F_S(k,t)$, which now incorporate the correct short-time ballistic limit.

The results for $W(t)$ and $F_S(k,t)$ for the atomic HS liquid are represented by the solid curves in Figs. 1(a) and 1(b), respectively. These results are plotted in terms of the MD "natural" (length and time) units, σ and $t_0 \equiv \sqrt{M\sigma^2/k_B T}$ at four values of the volume fraction $\phi = \pi n\sigma^3/6$, representative of the stable liquid regime, namely, $\phi = 0.3, 0.4, 0.45$, and 0.5. In the same figures, we have also included the corresponding

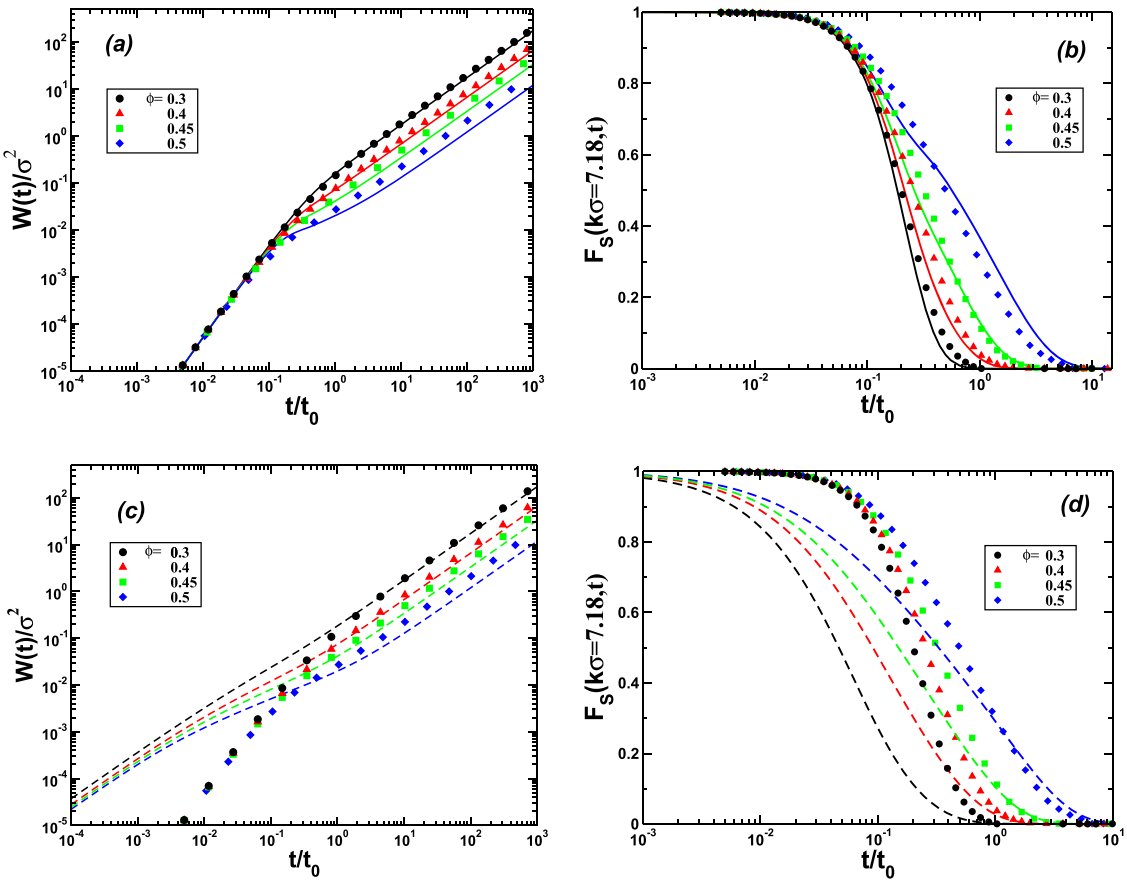

FIG. 1. Mean-square displacement $W(t)$ (in units of σ^2) and self-intermediate scattering function $F_S(k, t)$ of a hard sphere fluid as a function of the time t (in "molecular units" $t_0 = \sqrt{M\sigma^2/k_BT}$) for volume fractions $\phi = 0.3, 0.4, 0.45$, and 0.5. In all cases, symbols are the results of our MD simulations. The solid lines in (a) and (b) represent, respectively, the solution of Eq. (3.1) for $W(t)$ and Eq. (3.9) for $F_S(k, t)$ at a fixed wavevector $k\sigma = 7.18$. The dashed lines in (c) and (d) are the solutions of, respectively, Eqs. (2.13) and (2.11).

data (solid symbols) obtained by MD simulations. The details of the simulations are provided in Sec. IV. The comparison of Fig. 1(a) illustrates how, in spite of the fact that we have used the solution $\Delta\zeta^*(t)$ of the *overdamped* SCGLE theory to solve Eq. (3.1), the presence of the inertial term in the same equation ensures that the resulting MSD has the correct short-time limit $W(t) \approx v_0^2 t^2/2$ and correctly describes the passage of $W(t)$ from this ballistic regime to its long-time diffusive limit $W(t) \approx D_L t$. We observe that for volume fractions smaller than 0.5, the quality of the agreement is better than that observed at the volume fraction 0.5. For volume fractions in the metastable regime, $\phi \gtrsim 0.5$, these quantitative differences become larger (data not shown). In addition, deviations are also observed at intermediate times, which amplify slightly at the larger volume fractions. These inaccuracies, however, may be perfectly tolerable in a theory with a single adjustable parameter (see Eq. (2.12)).

For completeness, in Fig. 1(c) the solution of the *overdamped* version of Eq. (3.1) (see Eq. (2.13)) using the same *overdamped* $\Delta\zeta^*(t)$ as input has been included. The resulting MSD, represented by the dashed lines, describes the dynamics of the corresponding Brownian liquid whose solution satisfies the short- and long-time limits, i.e., $W(t \to 0) \approx D^0 t$ and $W(t \to \infty) \approx D_L t$, respectively. The comparison between the theoretical curves and the simulation data demonstrates the theoretically predicted long-time dynamic scaling between atomic and colloidal systems in the context of the MSD, as already reported in Ref. 25.

In Fig. 1(b) the theoretical predictions for $F_S(k, t)$ are compared with the corresponding MD results at the same volume fractions. This comparison indicates that the simple approximation in Eq. (3.9) provides a very good quantitative representation of $F_S(k, t)$ at very low volume fractions, although the inaccuracies of the theoretical results for $W(t)$ shown in Fig. 1(a) manifest themselves in the differences observed, particularly at $\phi = 0.5$ at intermediate times.

In Fig. 1(d), the quantitative differences between the solution of the overdamped SCGLEs (dashed lines) for $F_S(k, t)$ and the MD simulation data are illustrated. From this comparison, which complements the information provided in Fig. 1(b), one can see that throughout the low-density regime, the overdamped SCGLE theory fails in capturing the decay of the ISF at all (short, intermediate, and long) time scales. This is so because in this density regime of atomic liquids the decay of $F_s(k, t)$ is dominated by the microscopic short-time ballistic dynamics. It is only at high densities (near freezing) that the long-time (but not the short- and intermediate-time) decay of $F_s(k, t)$ of both atomic and Brownian liquids coincide. As explained in more detail in Fig. 2 of Ref. 24, this is due to the fact that at high densities the long-time decay of $F_s(k, t)$ of atomic liquids is now dominated by microscopic diffusive (not ballistic) processes.

Thus, one can conclude that the overdamped SCGLEs provide a good representation of the hard-sphere self-ISF at times longer than t_0, in particular, for volume fractions beyond a threshold value around $\phi \geq 0.45$. Below this threshold value, the overdamped SCGLE theory fails to capture the essentially ballistic decay of the ISF $F_S(k,t)$ of atomic liquids. This threshold coincides approximately with the freezing volume fraction and is actually the same as the crossover volume fraction referred to in Ref. 24, above which the dynamical equivalence between atomic and Brownian liquids is also exhibited by $F_S(k,t)$. The fact that this dynamical equivalence holds better when increasing the volume fractions in the metastable regime makes it specially relevant to understand the common phenomenology of colloidal and atomic glass formers, a point that will be addressed elsewhere.[46]

IV. SCGLE FORMALISM FOR *MULTICOMPONENT* ATOMIC LIQUIDS

We now describe the multicomponent extension of the SCGLE theory for atomic liquids. Since such an extension is in reality rather straightforward, we shall not go in any detail through each of the arguments reviewed in the monocomponent case. Instead, we only summarize the resulting set of SCGLEs that describe the dynamics of *multicomponent* atomic liquids and provide two illustrative applications involving the direct comparison with the corresponding MD simulation results. In this section, we also briefly describe the simulation methods employed.

A. Dynamics of multicomponent atomic liquids

Let us consider now an atomic liquid at temperature T inside a volume V and composed of N spherical particles belonging to ν different species (labeled by the index $i = 1, 2, \ldots, \nu$). Thus, $N = \sum_{i=1}^{\nu} N_i$, where N_i is the number of particles of the species i, each one having a mass M_i and a diameter σ_i. One can also define the number concentration of species i as $n_i \equiv N_i/V$. The relevant structural information of these multicomponent atomic liquids is contained in the elements $S_{ij}(k)$ of the $\nu \times \nu$ matrix $S(k)$ of partial static structure factors, whereas the most fundamental dynamical information is contained in the $\nu \times \nu$ matrices $F^D(k,t)$ and $F_S^D(k,t)$, whose elements are the collective and partial self-intermediate scattering functions $F_{ij}^D(k,t)$ and $\delta_{ij}F_{S,i}^D(k,t)$, respectively.

As explained in detail in Ref. 28, within the SCGLE formalism the time-evolution equations for the matrices $F^D(k,t)$ and $F_S^D(k,t)$, written in Laplace space, read as

$$F^D(k,z) = \{zI + k^2 D \cdot [zI + \lambda(k) \cdot \Delta\hat{\zeta}^*(z)]^{-1} \cdot S^{-1}(k)\}^{-1} \cdot S(k) \tag{4.1}$$

and

$$F_S^D(k,z) = \{zI + k^2 D \cdot [zI + \lambda(k) \cdot \Delta\hat{\zeta}^*(z)]^{-1}\}^{-1}, \tag{4.2}$$

where D and $\lambda(k)$ are diagonal matrices given by $D_{ij} \equiv \delta_{ij} D_i^0$ and $\lambda_{ij}(k) = \delta_{ij}[1 + (k/k_i^c)]^{-1}$ and with D_i^0 being the short-time self-diffusion coefficient of species i, which depends on the masses M_i, the temperature, and the size of the particles, in a manner that extends the monocomponent kinetic expression in Eq. (2.5). The parameter k_i^c is an empirical cut-off wavevector written as $k_i^c = a k_i^{max}$, in which k_i^{max} is the position of the maximum of $S_{ii}(k)$ and $a > 0$ is again the only free parameter, eventually determined by a calibration procedure.[43]

The ith diagonal element $\Delta\zeta_i^*(z)$ of the matrix $\Delta\hat{\zeta}^*(z)$ is the time-dependent friction function of particles of species i and according to Ref. 28 is given by

$$\Delta\zeta_i^*(t) = \frac{D_i^0}{3(2\pi)^3} \int d\mathbf{k}\, k^2 [F_S^D(t)]_{ii} [h \cdot \sqrt{n} \cdot S^{-1} \cdot F^D(t) \cdot S^{-1} \cdot \sqrt{n} \cdot h]_{ii}, \tag{4.3}$$

with the elements of the k-dependent matrix h given by $h = \sqrt{n^{-1}} \cdot (S - I) \cdot \sqrt{n^{-1}}$, where the elements of the matrix $\sqrt{n}$ are $[\sqrt{n}\,]_{ij} \equiv \delta_{ij}\sqrt{n_i}$, and we have systematically omitted the argument k of the $\nu \times \nu$ matrices $h(k)$, $S(k)$, $F^D(k,t)$, and $F_S^D(k,t)$.

Let us now write the corresponding results for the mean-square displacement, $W(t)$, with its diagonal elements, $W_i(t)$, i.e., the MSD of particles of species i, given by

$$\tau_i^0 \frac{dW_i(t)}{dt} + W_i(t) = D_i^0 t - \int_0^\tau \Delta\zeta_i^*(t - t') W_i(t') dt', \tag{4.4}$$

where $\tau_i^0 \equiv M_i/\zeta_i^0$ and with $\zeta_i^0 = k_B T/D_i^0$. Finally, the exponential interpolation functions for the $\nu \times \nu$ matrices $F(k,t)$ and $F_S(k,t)$ of a multicomponent atomic liquid can be written as

$$F(k,t) = F^D(k,t) + \{S(k) \cdot \exp[-k^2 W(t) \cdot S^{-1}(k)] - F^D(k,t)\} \cdot \exp[-Zt] \tag{4.5}$$

and

$$F_S(k,t) = F_S^D(k,t) + \{\exp[-k^2 W(t)] - F_S^D(k,t)\} \cdot \exp[-Zt], \tag{4.6}$$

where the diagonal matrix Z has non-zero elements $Z_i \equiv (\zeta_i^0/M_i)$.

Eqs. (4.1)–(4.6) thus extend to mixtures of the SCGLE formalism for an atomic liquid. In what follows, its use will be illustrated with two examples involving binary hard-sphere mixtures. The self-consistent solution of these equations requires the previous determination of the matrix $S(k)$ of partial static factors, which will be obtained using again the Percus-Yevick approximation for multicomponent[47] liquids and with the corresponding Verlet-Weiss correction ($\phi \to \phi - \phi^2/16$).[45,48] Once $S(k)$ has been determined, we solve Eqs. (4.1)–(4.3) to obtain the matrices $\Delta\zeta^*(t)$, $F^D(k,t)$, and $F_S^D(k,t)$, which describe the dynamics of the multicomponent atomic liquid in the diffusive or overdamped regime. We then use these results in Eqs. (4.4)–(4.6) to determine the MSD, $W(t)$, and the ISFs $F(k,t)$ and $F_S(k,t)$, which include the correct short-time ballistic regime.

B. Molecular dynamic simulations

As said in the Introduction, to test this SCGLE theory of the dynamics of atomic mixtures, we have carried out event-driven molecular dynamics simulations in the context of two

illustrative applications: a polydisperse HS liquid, modeled as a moderately size-asymmetric binary HS mixture, and a genuine, highly size-asymmetric binary HS mixture. Let us now briefly describe the simulation methods employed in each of these applications.

To simulate a polydisperse monocomponent HS liquid, we followed the methodology explained in Ref. 43, using *event-driven* MD simulations. The simulations were carried out with $N = 1000$ particles in a volume V. The diameters of these particles are uniformly distributed between $\overline{\sigma}(1 - w/2)$ and $\overline{\sigma}(1 + w/2)$, with $\overline{\sigma}$ being the average particle diameter. We have considered the case $w = 0.3$, which corresponds to a polydispersity $s_\sigma = w/\sqrt{12} = 0.0866$. We have assumed that all particles have the same mass M and the results are displayed in reduced units; therefore, $\overline{\sigma}$ and $\overline{\sigma}\sqrt{M/k_BT}$ are used as units of length and time, respectively. To improve the statistics and reduce the uncertainties, every correlation function is obtained over the average of 10 independent realizations for each volume fraction considered. The same protocol was employed to simulate the particular case of a monodisperse HS liquid ($w = 0$). In general, the effect of polydispersity on the dynamic properties $W(t)$ and $F_S(k, t)$ is not as dramatic as in the structure,[49] and the differences are even less noticeable in the stable liquid regime illustrated in Fig. 1,

In the case of highly asymmetric binary mixtures, we have carried out *event-driven* MD simulations for a HS binary system with an asymmetry parameter $\delta \equiv \sigma_s/\sigma_b = 0.2$. Here the labels s and b correspond, respectively, to *small* and *big*. Thus, we have simulated a system of $N(= N_b + N_s)$ particles, consisting of N_b *big* particles and N_s *small* particles, in a volume V. More specifically, we have considered three different state points in the control parameter space of the system spanned by the pair (ϕ_b, ϕ_s), where $\phi_i = \pi n_i \sigma_i^3/6$ and $n_i = N_i/N$ $(i = b, s)$. Given N_b, the size of the cubic simulation box was adjusted in order to control ϕ_b. Then, N_s was adjusted to control ϕ_s (see Ref. 46). The specific simulated state points were **I** = (0.45, 0.05), with $N_b = 200$ and $N_s = 2778$; **II** = (0.45, 0.2), with $N_b = 150$ and $N_s = 8333$; and **III** = (0.6, 0.05), with $N_b = 200$ and $N_s = 2083$. For the state points **I** and **III**, 10 realizations of the system were performed, i.e., runs with 10 different *seeds* have been used to explore the available phase space and to improve the statistics. For the state point **II**, 5 different *seeds* have been considered. In these simulations, the unit of length is defined by the diameter of the large particles, σ_b, and the unit of mass is defined as the mass of the big particles, M_b. The mass densities, $\rho_i^M \equiv M_i/v_i$ $(v_i = 4\pi\sigma_i^3/3, i = s, b)$, are set equal to define the mass of the small particles. Setting $k_B = 1$, the unit of time is defined from the equipartition theorem $\langle v_b^2 \rangle = 3k_BT/M_b$. Periodic boundary conditions were employed in all directions. It is also worth stressing that for the points **I** and **II** we have used a *waiting* time $t_w = 10^3$, while for **III** we let $t_w = 10^4$, in order to avoid aging effects (see Ref. 46). Finally, it should be mentioned that in order to generate non-overlapping initial configurations, a soft-core standard molecular dynamics with a repulsive short-range potential and decreasing temperature was implemented.[50] This soft-core MD starts from a completely random initial configuration.

C. Polydisperse hard-sphere atomic liquid

Let us now proceed to solve the SCGLE, Eqs. (4.1)–(4.6), for the first of the two examples just described, namely, a polydisperse HS liquid with uniform size distribution and polydispersity $s_\sigma = 0.0866$. We can model this distribution with its discretized version by partitioning the interval $\overline{\sigma}(1 - w/2) \le \sigma \le \overline{\sigma}(1 + w/2)$ in ν equally sized bins and treat the polydisperse liquid as a ν-component mixture. To compare with the simulations, we then compute the total properties, such as $W(t) \equiv \sum_{i=1}^{\nu} x_i W_i(t)$, $F(k;t) = \sum_{i,j=1}^{\nu} \sqrt{x_i x_j} F_{ij}(k,t)$, and $F_S(k,t) \equiv \sum_{i=1}^{\nu} x_i F_i^S(t)$, where $W_i(t)$, $F_{ij}(k, t)$, and $F_i^S(t)$ are the partial MSD, collective ISFs, and self ISFs of the mixture, and where $x_i = n_i/\sum_{i=1}^{\nu} n_i$.

To solve Eqs. (4.1)–(4.6), we need first to determine its static input, i.e., the partial static structure factors, but as said above, for our HS system these will be provided by the multicomponent Percus-Yevick approximation with its Verlet-Weiss correction.[45,47,48] We also need to previously determine the short-time self-diffusion coefficients D_i^0 $(i = 1, 2 \ldots \nu)$. Unfortunately, the random-flight arguments involved in the derivation of the monocomponent kinetic-theoretical expression in Eq. (2.5) are not easily generalized to the case of an arbitrary ν-component atomic liquid. Thus, if we do not wish to treat these as free adjustable parameters, we must resort to additional approximations or simplifications, as we do in the present application.

Thus, to model the simulated HS polydisperse liquid, let us use the approach just described in its simplest form, i.e., by considering an equimolar HS binary mixture, with components having number concentrations $n_1 = n_2 = n_t/2$ and particle diameters $\sigma_1 = \overline{\sigma}(1 - \epsilon)$ and $\sigma_2 = \overline{\sigma}(1 + \epsilon)$, with $\epsilon = 0.0866$ chosen such that the mean diameter, $\bar{\sigma}$, and mean-square diameter, $\bar{\sigma^2}$ (and hence, the polydispersity), are the same as that of the simulated system. Furthermore, given the small asymmetry between the constituent particles ($\delta \approx 0.84$), it is reasonable to approximate the short-time self-diffusion coefficients D_1^0 and D_2^0 as $D_1^0 = D_2^0 = D_{eff}^0$, where D_{eff}^0 is the short-time self-diffusion coefficient of an effective monodisperse system with concentration n_t and diameter $\bar{\sigma}$, given by (see Eq. (2.5))

$$D_{eff}^0 \equiv \frac{3}{8}\left(\frac{k_BT}{\pi M}\right)^{1/2} \frac{1}{n_t \bar{\sigma}^2}. \tag{4.7}$$

As it is shown in what follows, this proposal allows us to provide a good representation of the referred dynamical properties of the simulated polydisperse fluid.

In Fig. 2 we show the theoretical predictions for $W(t)$ and $F_S(k, t)$ compared against the corresponding MD simulation results for a set of volume fractions. Fig. 2(a) illustrates how, using the *overdamped* friction functions $\Delta\zeta_i^*(t)$ in the time-evolution equations for $W_i(t)$ (Eq. (4.4)) and assuming $D_1^0 = D_2^0 = D_{eff}^0$, an effective MSD (solid lines) is generated, which nicely describes the ballistic regime, although some quantitative differences appear at long times. Such deviations, however, should be expected considering the calibration procedure employed to fix the only phenomenological parameter of the SCGLE theory, namely, the cutoff wavevectors k_i^c $(i = 1, \ldots, \nu)$. These were first reduced to a single

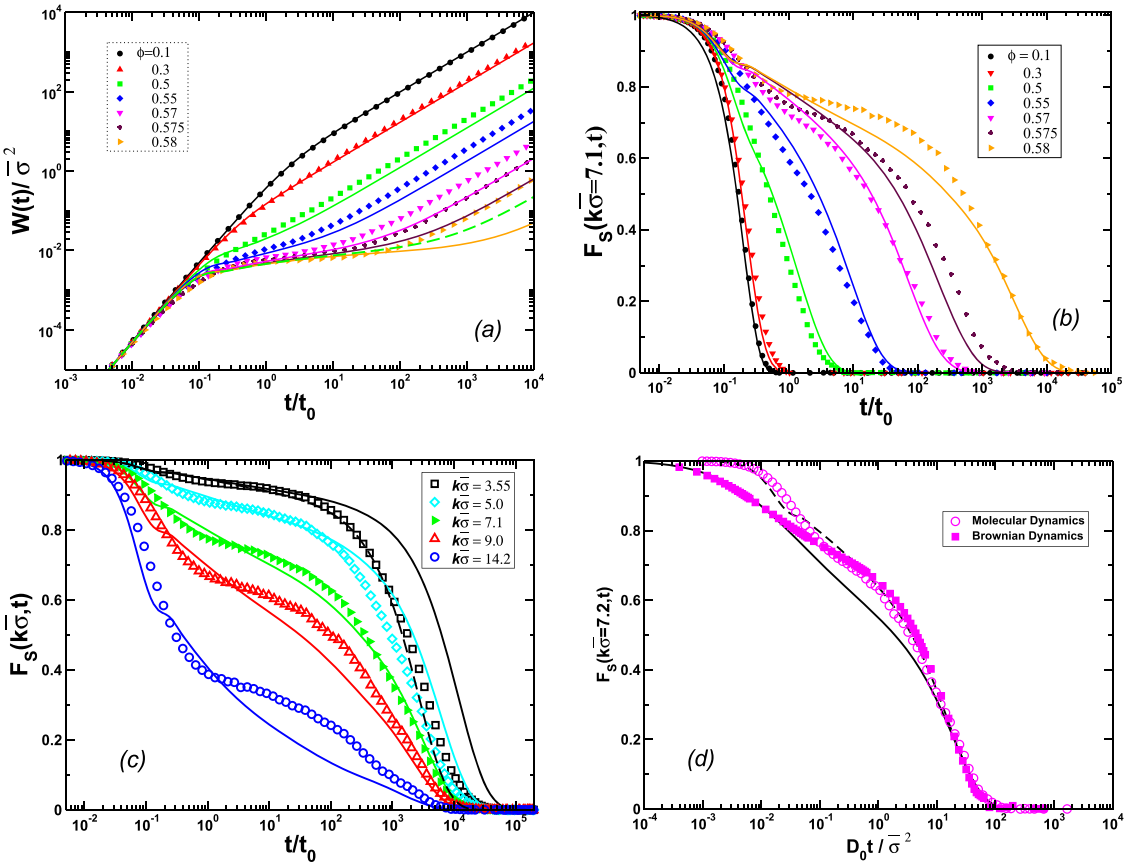

FIG. 2. (a) Mean-square displacement $W(t)$ and (b) self-ISF, $F_S(k,t;\phi)$, at fixed $k\bar{\sigma} = 7.1$, as a function of time t (in "molecular" units $t_0 \equiv \bar{\sigma}\sqrt{M/k_BT}$) for the polydisperse hard-sphere atomic liquid (polydispersity = 8.66%) at the indicated volume fractions. (c) Behaviour of the self-ISF, $F_S(k,t;\phi)$, at several wavevectors and fixed volume fraction $\phi = 0.58$. In all figures, symbols represent the MD simulations data and the solid lines are the predictions of the SCGLE formalism for atomic liquids. The dashed line in (a) and (c) corresponds to the value $k_c = 8.1$ of the cutoff wave-vector k_c for the volume fraction $\phi = 0.58$, to illustrate an alternative calibration of this free parameter of the SCGLE theory (see discussion in the main text). (d) Molecular dynamics (empty symbols) and Brownian dynamics (solid symbols) simulation results for the self-intermediate scattering function $F_S(k,t)$ at $\phi = 0.571$, evaluated at $k\bar{\sigma} = 7.2$, and plotted as a function of the dimensionless time $D_0t/\bar{\sigma}^2$ (see discussion in the main text), the solid and dashed lines represent the theoretical predictions of the colloidal and the atomic SCGLE theory, respectively.

parameter, $k_i^c = k_c$, and then their value was determined as $k_c = 8.2$ by requiring the best *overall* (i.e., for all ϕ's) fit of the theory with the simulation data for the so-called α-relaxation time $\tau^{(\alpha)}$, defined by $F_S(k\bar{\sigma}, t = \tau^{(\alpha)}) = e^{-1}$. This exercise was performed at the wave-vector $k\bar{\sigma} = 7.1$. For this reason, the *overall* long-time agreement with the simulation results of the predicted $F_S(k, t)$ (see Fig. 2(b)) is in general better than that of $W(t)$. One observes, however, that the quality of the agreement between the predicted and the simulated $F_S(k, t)$ at short and long times is better for volume fractions smaller than 0.5 than in the metastable regime, $\phi \gtrsim 0.5$.

Regarding the accuracy of the theory at different wave-vectors, this is illustrated in Fig. 2(c). There we compare the theoretical and simulated $F_S(k, t)$ for a set of wave-vectors larger and smaller than 7.1, keeping fixed the same value $k_c = 8.2$. This figure also illustrates that the overall qualitative trends of the simulations are accurately captured by the theoretical results, at least at a level that one should expect from an approximate theory involving a single fitting parameter, while varying a wide range of volume fractions and wave-vectors.

A still more relevant point is the expectation that the accuracy of the theory would diminish for smaller wavevectors, since then the Gaussian approximation $F_s(k;t) = \exp[-k^2W(t)/6]$ is exact and our predictions for $W(t)$ are quantitatively less accurate at long times. As also observed in Fig. 2(c), the difference between theory and simulation certainly increases for decreasing wave-vectors. This means that if we wish to improve the accuracy of the predicted $W(t)$, it is better to determine k_c not at the peak of $S(k)$ but at a smaller wave-vector. To check this expectation, we determined the value of k_c that provides the best fit of $F_S(k\bar{\sigma} = 3.55, t)$ (dashed line in Fig. 2(c)), yielding $k_c = 8.1$. Although this leads to a poorer accuracy of the predicted $F_S(k, t)$ at large wave-vectors, it does lead to a sensible improvement of the accuracy of the predicted $W(t)$ (dashed line of Fig. 2(a)).

Let us finally notice that the initial decay to the incipient plateau strongly depends on the microscopic dynamics and that this feature is correctly captured by the SCGLE theory. To illustrate this in Fig. 2(d), we present a comparison of the overdamped *vs.* atomic ISFs for the HS liquid at $\phi = 0.571$, along with the corresponding Brownian *vs.* molecular dynamics (MD) simulation data. These data are essentially those in Fig. 2(a) of Ref. 24, which discusses in all detail the difference in the initial, short-time, decay (or beta-relaxation) of the intermediate scattering function (ISF) $F_S(k, t)$ depending on the microscopic dynamics. The same reference also discusses the expected collapse of both results for the ISF at long times

when plotted as a function of the time scaled as $D_0 t/\sigma^2$, with D_0 given by the expression in Eq. (4.7) above.

In Fig. 2(d), however, we have also included the corresponding intermediate scattering function $F_S(k = 7.2, t)$ predicted by the colloidal SCGLE theory (solid line) and by the atomic SCGLE theory introduced in the present paper (dashed line). From the comparisons in this figure, one can appreciate how the main differences in the Brownian vs. molecular dynamics simulations are correctly (although not perfectly) captured by the comparison between the colloidal vs. atomic SCGLE approach. In this way, the main message of this figure is that the overdamped (or colloidal) SCGLE theory is to be compared with Brownian dynamics simulation, whereas the atomic SCGLE theory developed here is to be compared with molecular dynamics simulations.

D. Highly size-asymmetric binary mixture

The previous example illustrates a simple manner to apply the SCGLE theory of atomic mixtures to represent the dynamical properties of a polydisperse fluid. The small degree of polydispersity allowed us to use the approximation $D_1^0 = D_2^0 = D_{eff}^0$. Let us now turn our attention to the case of highly asymmetric HS binary mixtures, illustrated with the simulated mixture with size asymmetry $\delta = 0.2$ (and mass asymmetry $M_s/M_b = \delta^3 = 0.008$). The theoretical procedure is exactly the same, except that now we need to keep a track of the partial dynamic properties $W_i(t)$, $F_{ij}(k, t)$, and $F_i^S(t)$, and the size- and mass-asymmetries are much larger. This forces one to consider more accurate expressions for the short-time diffusion coefficients D_1^0 and D_2^0 provided by kinetic theory, namely,[10]

$$D_b^0 = \frac{3}{2}\left(\frac{k_B T}{\pi M_b}\right)^{1/2}\left[\frac{1}{4\sigma_b^2 n_b + (\sigma_b+\sigma_s)^2 n_s}\right], \tag{4.8}$$

$$D_s^0 = \frac{3}{2}\left(\frac{k_B T}{\pi M_s}\right)^{1/2}\left[\frac{1}{(\sigma_b+\sigma_s)^2 n_b + 4\sigma_s^2 n_s}\right], \tag{4.9}$$

which contain the monocomponent expression in Eq. (2.5) as a particular case.

In practice, however, since the big particles are far more massive than the small particles, in determining the self-diffusion coefficient of the large spheres, we simply assume that the most representative collisions contributing to D_b^0 are those among big particles, and thus, we may approximate such coefficients by (see Eq. (2.5))

$$D_b^0 \equiv \frac{3}{8}\left(\frac{k_B T}{\pi M_b}\right)^{1/2}\frac{1}{n_b\sigma_b^2}. \tag{4.10}$$

For the small particles, however, we do consider both types of collisions, i.e., those involving only small particles and those among small and large ones, so that

$$\frac{D_s^0}{D_b^0} = 4\left(\frac{M_b}{M_s}\right)^{1/2}\left[\frac{\sigma_b^2 n_b}{(\sigma_b+\sigma_s)^2 n_b + 4\sigma_s^2 n_s}\right]. \tag{4.11}$$

To test the accuracy of the resulting approximate theory, we have solved Eqs. (4.4)–(4.6) with Eqs. (4.10) and (4.11) for the MSDs, $W_i(t)$, and self-ISFs, $F_i^S(t)$ of the highly asymmetric binary HS mixture ($\delta = 0.2$) for three aforementioned state points in the high-concentration region of the control parameter space (ϕ_b, ϕ_s), namely, **I** = (0.45, 0.05), **II** = (0.45, 0.2), and **III** = (0.60, 0.05). The corresponding predictions are compared in Fig. 3 with their simulation counterparts. The first bird-eye conclusion of this comparison is that the theory provides quite a reasonable representation of the simulation results, considering its approximate nature and the simplicity of its underlying approximations and simplifications.

More quantitatively, we notice that the theoretical results exhibit the correct short- and long-time behavior of $W_i(t)$, including the disparate time scales of the dynamics of $W_b(t)$ and $W_s(t)$ when plotted as a function of the scaled time t_m (defined in units of σ_b and M_b). This time scale difference originates in the huge mass ratio $M_s/M_b = \delta^3 = 0.008$. This can be seen through the short-time (ballistic) solution of Eq. (4.4), $\langle(\Delta\mathbf{r}_i(t))^2\rangle \approx [3k_BT/M_i]t^2$ which, expressed in terms of $W_i(t) = \langle(\Delta\mathbf{r}_i(t))^2\rangle/6$, reads as

$$\frac{W_i(t_m)}{\sigma_b^2} = \frac{1}{2}\left[\frac{M_b}{M_i}\right](t_m)^2, \tag{4.12}$$

where $t_m \equiv t/t_b^0$ and $t_b^0 = \sigma_b\sqrt{M_b/k_BT}$. The ratio $[M_b/M_i]$ is unity for the big particles ($i = b$) and is 0.008 for the small particles ($i = s$), thus explaining the aforementioned time scale difference.

Figs. 3(a)–3(f) correspond, respectively, to the points **I**, **II**, and **III**. These figures illustrate the effect on the dynamics of the system upon variations in the two control parameters ϕ_b and ϕ_s. For instance, regarding the dynamics of the system at the state point **I** = ($\phi_b = 0.45, \phi_s = 0.05$), one notices that, besides the aforementioned time scale difference in the MSDs of both species observed in Fig. 3(a), the SCGLE results for the ISFs of each species in Fig. 3(b) (solid and dashed lines) also reveal a noticeable difference between the characteristic decay times of the ISFs of each species, although the one-step relaxation pattern of each correlator is rather similar. The differences in the decay times are described by the α-relaxation times, $\tau_i^{(\alpha)}$ ($i = b, s$), defined here as $F_i^S(k\sigma_b = 7.18; \tau_i^{(\alpha)}) = 1/e$. These features are consistent with the results obtained from MD simulations (solid and open symbols).

Upon increasing ϕ_s from 0.05 to 0.2, we go from state point **I** to state point **II** = (0.45, 0.2), and in Figs. 3(c) and 3(d) we observe that the mobility of both species decreases. In addition, the crossover from the ballistic to the diffusive regime occurs at shorter times compared with the situation illustrated at **I**, and the difference between the corresponding α-relaxation times becomes larger. The simulation results nicely confirm these trends.

A more interesting behavior is observed when we move from state point **I** to state point **III** = (0.6, 0.05), this time by fixing $\phi_s = 0.05$ and increasing ϕ_b from 0.45 to 0.6, above the glass transition threshold $\phi^{(g)} \approx 0.582$ of the monodisperse HS fluid. As illustrated in Figs. 3(e) and 3(f), in addition to the different time scales of $W_b(t)$ and $W_s(t)$ derived from

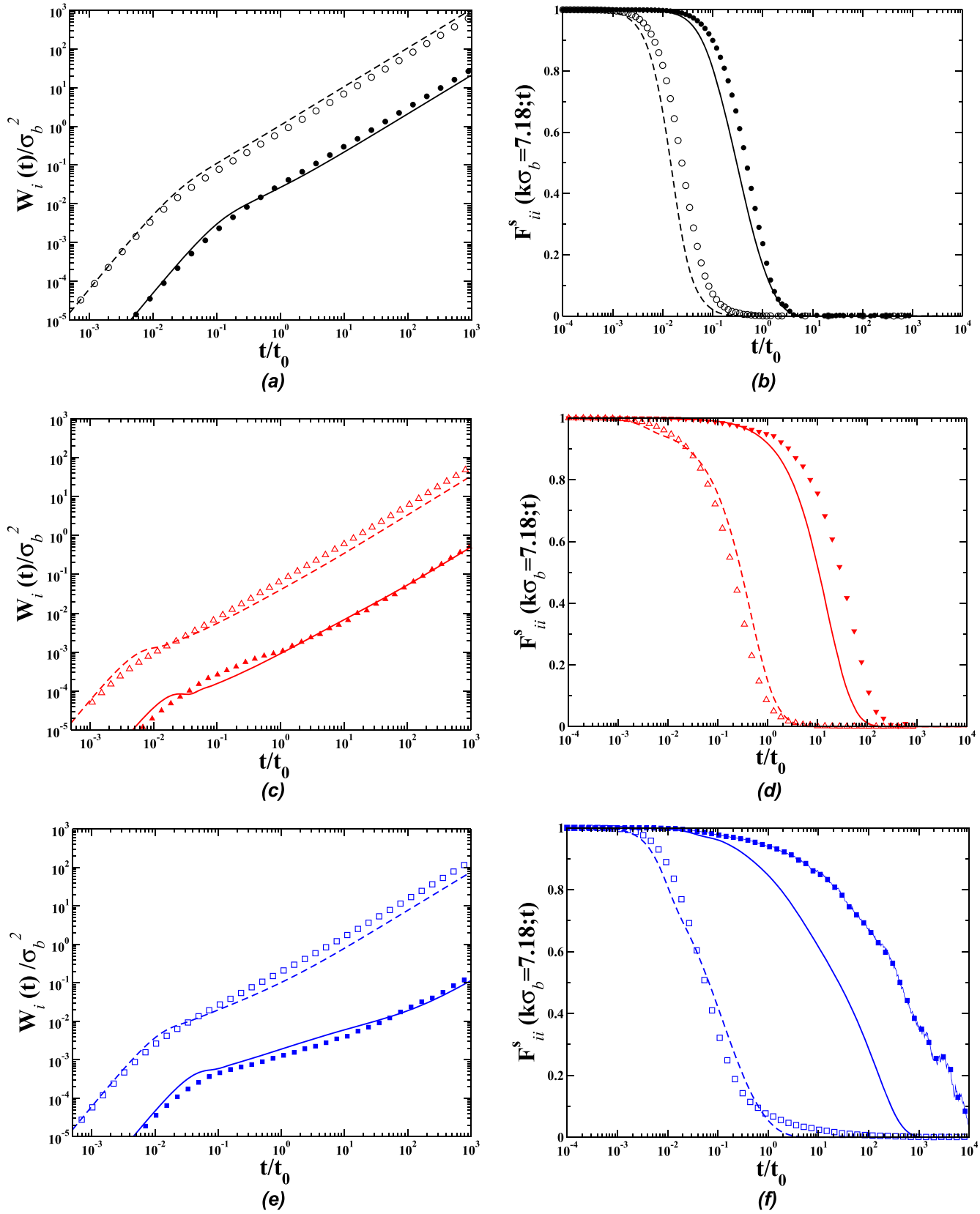

FIG. 3. Theoretical (solid and dashed lines) and simulation (solid and open symbols) results for the MSDs, $W_i(t)$, and ISFs $F_i^s(k = 7.18; t)$ of a highly asymmetric ($\delta = 0.2$) binary mixture of HS, for the three volume fractions, in the control parameter space (ϕ_b, ϕ_s). (a) and (b) correspond to the point **I** = (0.45, 0.05). (c) and (d) correspond to **II** = (0.45, 0.2). (e) and (f) correspond to **III** = (0.60, 0.05). In all cases, solid symbols (●,▲, ■) and solid lines correspond to the dynamical properties of big particles, whereas empty symbols (○, △, □) and dashed lines account for small particles.

the disparate mass difference, a further enhancement of this difference is now quite visible at long times, suggesting a strong disparity in the structural relaxation of the two species. For instance, a large disparity in the mobility of each species, measured by the ratio $W_b(t_m = 10^3)/W_s(t_m = 10^3) \sim 10^{-3}$, is observed. Note also the emergence of an incipient plateau in

the MSD of the large particles, which is absent in the MSD of the small ones.

Let us also notice that within the time-window of Fig. 3(e), theory and simulations coincide in which the mean-square displacement $W_b(t)$ of the big particles is not yet linear in t. Although not illustrated in the figure, we can mention that for longer times (clearly beyond the time-window of the figure), the SCGLE theory does predict linearity, with a small value of the long-time self-diffusion coefficient D_b^L. This subdiffusive behavior is actually indicative of the proximity to a dynamic arrest transition in which the theory predicts that the diffusion coefficient of the big particles, D_b^L, will vanish (see Ref. 46). In fact, such a predicted transition line can be crossed if we fix $\phi_s = 0.05$ and increase ϕ_b from 0.60 to a critical value $\phi_b = 0.638$. Thus, in the space state (ϕ_b, ϕ_s) of the binary mixture, this dynamic arrest transition separates the region of fully ergodic states (where both D_b^L and D_s^L are finite) from a region of mixed states, in which the big particles are predicted to form an amorphous solid (a glass, with $D_b^L = 0$), with the small particles still diffusing ($D_s^L > 0$) through the voids left by this amorphous structure. This long-time dynamic asymmetry is also observed in the ISFs of each species, which display different relaxation patterns, characterized by a faster relaxation mechanism for the small particles and a far slower relaxation of the large particles. Except for quantitative details, mostly manifested in $F_{bb}^S(k,t)$, the comparison with the simulation data demonstrates that these theoretical predictions capture the essential phenomenology of the simulation results. However, dwelling deeper into the description and understanding of this phenomenology will be discussed in more detail in a separate work.[46]

V. CONCLUDING REMARKS

In this paper, we have proposed and tested an approximate but quantitative theoretical approach for the description of the dynamics of *fully equilibrated* atomic liquid mixtures. Such a framework was built on the exact time-evolution equations for the long-time dynamics of an atomic liquid, previously developed in Refs. 23–25, which were complemented by a set of well-defined approximations, including a Gaussian-like approximation that incorporates the correct ballistic short-time limit. The predictive accuracy of the resulting theoretical tool was confirmed with the assistance of pertinent molecular dynamic simulations. The general conclusion drawn from these numerical tests indicate a remarkable degree of reliability of the present SCGLE theory. Although its quantitative accuracy could be improved in several manners, this was not the primary interest of the present work. Here we focused, instead, in illustrating the systematic use of our theory in two representative and concrete examples. The first involved a simple but polydisperse HS liquid and the second a genuine and highly asymmetric binary mixture of hard spheres.

In both cases, we expect that the present approximate theory will evolve into a useful theoretical tool to model the properties of experimentally relevant atomic liquid mixtures, such as molten salts and metallic alloys. This unification of the physics of colloidal and atomic liquids clearly creates an opportunity to systematically transfer much of the knowledge generated in the field of colloids to the understanding of complex atomic liquid mixtures and vice versa. For instance, both examples discussed here actually derive from two separate projects involving model colloidal HS liquids, whose properties could in practice be more easily simulated using event-driven molecular dynamics, rather than the more natural Brownian dynamics simulations. In the first example, since hard-sphere colloids are usually polydisperse, theoretically describing polydispersity with the SCGLE theory and then testing the results with MD simulations is now a natural and handy modeling protocol, as discussed in more detail elsewhere.[51] The same protocol is being followed in modeling the dynamics of genuine HS colloidal mixtures with large size asymmetry and discussed in more detail in a separate work.[46]

Finally, another particularly relevant opportunity is represented by the possibility of connecting the advances in our understanding of the formation of colloidal glasses and gels with the technologically relevant need to understand the formation of amorphous solids by the cooling of complex glass- and gel-forming atomic liquids. Although this more ambitious project requires the development of the non-equilibrium version of the present SCGLE theory of equilibrium atomic liquids, the present work paves the way for such developments.

ACKNOWLEDGMENTS

The authors acknowledge Dr. Leticia López-Flores for kindly providing the simulation data of Fig. 2(d). This work was supported by the Consejo Nacional de Ciencia y Tecnología (CONACYT, México) through Grant Nos. 242364, 182132, 237425, 358254, and FC-2015-2/1155 and by the Universidad de Guanajuato (through the Convocatoria Institucional para el Fortalecimiento de la Excelencia Académica 2015). P.E.R.G. acknowledges financial support from Cátedras CONACyT Nos. 1631 and CB-2015-01 No. 257636. G.P.A. acknowledges the support of Cluster de Supercomputo KUKULCAN, Conacyt (Grant No. CB-2015-252356). L.F.E.A. and R.C.P. acknowledge financial support from Secretaría de Educación Pública (SEP, México) through Postdoctoral fellowship, PRODEP. P.M.M. and M.M.N. acknowledge the support of Secretaría de Educación Pública through postdoctoral fellowship, PRODEP. L.F.E.A. also acknowledges financial support from the German Academic Exchange Service (DAAD) through the DLR-DAAD programme under Grant No. 212. R.C.P. also acknowledges the financial support provided by the Marcos Moshinsky Fellowship No. 2013 - 214 and the Alexander von Humboldt Foundation during his stay at the University of Düsseldorf in summer 2016. The authors acknowledge Thomas Voigtmann for interesting discussions.

[1] J. P. Boon and S. Yip, *Molecular Hydrodynamics* (McGraw-Hill, New York, 1980).
[2] U. Balucani and M. Zoppi, *Dynamics of the Liquid State* (Oxford University Press, New York, 1994).
[3] S. K. Das, J. Horbach, M. M. Koza, S. M. Chathoth, and A. Meyer, Appl. Phys. Lett. **86**, 011918 (2005).

[4]F. Yang, D. Holland-Moritz, J. Gegner, P. Heintzmann, F. Kargl, C. C. Yuan, G. G. Simeoni, and A. Meyer, Europhys. Lett. **107**, 46001 (2014).
[5]P. N. Pusey and W. van Megen, Nature **320**, 340 (1986).
[6]P. N. Pusey and W. van Megen, Phys. Rev. Lett. **59**, 2083 (1987).
[7]P. N. Pusey and W. V. Megen, Phys. A **157**, 705 (1989).
[8]I. M. de Schepper, E. G. D. Cohen, P. N. Pusey, and H. N. W. Lekkerkerker, J. Phys.: Condens. Matter **1**, 6503 (1989).
[9]P. N. Pusey, H. N. W. Lekkerkerker, E. G. D. Cohen, and I. M. de Schepper, Phys. A **164**, 12 (1990).
[10]D. A. McQuarrie, *Statistical Mechanics* (Harper and Row, New York, 1975).
[11]J. P. Hansen and I. R. McDonald, *Theory of Simple Liquid* (Academic Press, Inc., 1976).
[12]G. Nägele, Phys. Rep. **272**, 215 (1996).
[13]P. N. Pusey in *Liquids, Freezing and Glass Transition*, edited by J. P. Hansen, D. Levesque, and J. Zinn-Justin (Elsevier, Amsterdam, 1991), Chap. 10.
[14]W. van Megen and S. M. Underwood, Phys. Rev. E **49**, 4206 (1994).
[15]W. van Megen, T. C. Mortensen, S. R. Williams, and J. Müller, Phys. Rev. E **58**, 6073 (1998).
[16]G. Szamel and H. Löwen, Phys. Rev. A **44**, 8215 (1991).
[17]H. Löwen, J. P. Hansen, and J. N. Roux, Phys. Rev. A **44**, 1169 (1991).
[18]T. Gleim, W. Kob, and K. Binder, Phys. Rev. Lett. **81**, 4404 (1998).
[19]G. Szamel and E. Flenner, Europhys. Lett. **67**, 779 (2004).
[20]A. M. Puertas, J. Phys.: Condens. Matter **22**, 104121 (2010).
[21]L. López-Flores, P. Mendoza-Méndez, L. E. Sánchez-Díaz, L. L. Yeomans-Reyna, A. Vizcarra-Rendón, G. Pérez-Ángel, M. Chávez-Páez, and M. Medina-Noyola, Europhys. Lett. **99**, 46001 (2012).
[22]M. Medina-Noyola, Faraday Discuss. Chem. Soc. **83**, 21 (1987).
[23]P. Mendoza-Méndez, L. López-Flores, A. Vizcarra-Rendón, L. E. Sánchez-Díaz, and M. Medina-Noyola, Phys. A **394**, 1 (2014).
[24]L. López-Flores, L. L. Yeomans-Reyna, M. Chávez-Páez, and M. Medina-Noyola, J. Phys.: Condens. Matter **24**, 375107 (2012).
[25]L. López-Flores, H. Ruíz-Estrada, M. Chávez-Páez, and M. Medina-Noyola, Phys. Rev. E **88**, 042301 (2013).
[26]R. Juárez-Maldonado *et al.*, Phys. Rev. E **76**, 062502 (2007).
[27]M. A. Chávez-Rojo and M. Medina-Noyola, Phys. Rev. E **72**, 031107 (2005); **76**, 039902 (2007).
[28]R. Juárez-Maldonado and M. Medina-Noyola, Phys. Rev. E **77**, 051503 (2008).
[29]W. Götze, in *Liquids, Freezing and Glass Transition*, edited by J. P. Hansen, D. Levesque, and J. Zinn-Justin (North-Holland, Amsterdam, 1991).
[30]W. Götze and L. Sjögren, Rep. Prog. Phys. **55**, 241 (1992).
[31]J. Bosse and J. S. Thakur, Phys. Rev. Lett. **59**, 998 (1987).
[32]J. L. Barrat and A. Latz, J. Phys.: Condens. Matter **2**, 4289 (1990).
[33]G. Nägele, J. Bergenholtz, and J. K. G. Dhont, J. Chem. Phys. **110**, 7037 (1999).
[34]F. Weysser, A. M. Puertas, M. Fuchs, and Th. Voigtmann, Phys. Rev. E **82**, 011504 (2010).
[35]W. Kob, M. Nauroth, and F. Sciortino, J. Non-Cryst. Solids **307-310**, 181 (2002).
[36]Th. Voigtmann, A. Meyer, D. Holland-Moritz, S. Stüber, T. Hansen, and T. Unruh, Europhys. Lett. **82**, 66001 (2008).
[37]C. A. Angell, K. L. Ngai, G. B. McKenna, P. F. McMillan, and S. F. Martin, J. Appl. Phys. **88**, 3113 (2000).
[38]P. E. Ramírez-González and M. Medina-Noyola, Phys. Rev. E **82**, 061503 (2010).
[39]L. E. Sánchez-Díaz, P. E. Ramírez-González, and M. Medina-Noyola, Phys. Rev. E **87**, 052306 (2013).
[40]J. M. Olais-Govea, L. López-Flores, and M. Medina-Noyola, J. Chem. Phys. **143**, 174505 (2015).
[41]G. E. Uhlenbeck and L. S. Ornstein, Phys. Rev. **36**, 823 (1930).
[42]L. Yeomans-Reyna and M. Medina-Noyola, Phys. Rev. E **62**, 3382 (2000).
[43]G. Pérez-Ángel, L. E. Sánchez-Díaz, P. E. Ramírez-González, R. Juárez-Maldonado, A. Vizcarra-Rendón, and M. Medina-Noyola, Phys. Rev. E **83**, 060501(R) (2011).
[44]J. K. Percus and G. J. Yevick, Phys. Rev. **110**, 1 (1957).
[45]L. Verlet and J.-J. Weis, Phys. Rev. A **5**, 939 (1972).
[46]L. F. Elizondo-Aguilera, E. Lázaro-Lázaro, J. A. Perera-Burgos, G. Pérez-Ángel, M. Medina-Noyola, and R. Castañeda-Priego (unpublished).
[47]R. J. Baxter, J. Chem. Phys. **52**, 4559 (1970).
[48]S. R. Williams and W. van Megen, Phys. Rev. E **64**, 041502 (2001).
[49]E. Zaccarelli, C. Valeriani, E. Sanz, W. C. K. Poon, M. E. Cates, and P. N. Pusey, Phys. Rev. Lett. **103**, 135704 (2009).
[50]M. C. Vargas and G. Pérez-Ángel, Phys. Rev. E. **87**, 042313 (2013).
[51]P. Mendoza-Méndez, E. Lázaro-Lázaro, L. E. Sánchez-Díaz, P. E. Ramírez-González, G. Pérez-Ángel, and M. Medina-Noyola (unpublished).